In-doped ZnO nanorods prepared by electrochemical deposition route

J. X. GONG, Y. T. DAI*, H. ZHANG, L. Y. PU, W. WANG
School of Materials Science and Engineering, Southwest University of Science and Technology, Mianyang 621010, China

In-doped ZnO nanorods on the ITO glass substrate were successfully obtained by electrochemical deposition route. The morphology and size of the nanorods were studied by controlling contents of indium and the deposition potentials. The results of EDX and XRD both proved that these prepared nanorods are indeed composed of wurtzite structure In-doped ZnO crystals. The HRTEM revealed that the nanorods obtained the preferential growth along [0001] direction and those nanorods consist of single crystals. The PL spectra of In-doped ZnO nanorods coated on ITO glass substrate appeared markedly red-shifted by increasing contents of indium at the peak about 371 nm.

(Received November 15, 2017; accepted November 29, 2018)

Keywords: In-doped ZnO nanorod, Electrodeposition, Dispersed element, PL

1. Introduction

As a new type multifunction inorganic material, nano-ZnO has wide application prospect in many fields. Present interest on the development of nano-ZnO devices for catalytic [1], optical [2], optoelectronic [3], electrical [4], and other applications have a huge thrust on the development of nanoelectronic devices. Many researchers are interested in the study of the mechanism of nano-ZnO, so as to improve its performance in some aspects. For example, Tang and Tian research shows that a high proportion (0001) facets of ZnO photocatalyst showed high photocatalytic properties, this is mainly due to the hydroxyl ions more prone to adsorption on the (0001) crystal surface, can generate hydroxyl radicals and whole reaction, thus improving the photocatalytic activity [5].

It is well known that take advantage of intrinsic lattice defects for chemical doping can make greatly influence of electronic, optical, magnetic and catalytic properties of ZnO [6-8]. Therefore, the zinc oxide can be doped with an element to enhance its optical, electrical, magnetic and catalytic properties. For example, ZnO doped with group V (N, P, As) can affect the its conductivity, making n-type ZnO into p-type, and band gap with the increase in voltage decreases [9-11]. Doped with group III (Al, Ga, In) can improve the optical properties of ZnO [12-14]. ZnO has been doped with the appropriate concentration of transition metal ions (Fe^{3+} , Cu^{2+} , Co^{2+} ,Ni^{2+} ,Mn^{2+}) can enhance its photocatalytic activity [15-18]. Recently, researchers have focused on the application of semiconductor materials doped with dispersed element as optoelectronic devices [19-22]. The optical, magnetic, and electrical capabilities of dispersed element doped nano-ZnO were decided by its crystal structure, contents of dopant, preparation methods, and preparation conditions.

Different properties of ZnO nanostructures have been prepared by various synthesis processes, such as pulsed laser deposition [23], sol-gel technique [24], magnetron sputter deposition [25], wet chemical etching [26], hydrothermal route [27], and molecular beam epitaxy [28]. In this paper, we chose an electrochemical deposition process for preparation of In-doped ZnO nanorods. The electrochemical deposition is a simple, quick and inexpensive technique, In-doped ZnO nanorods have been successfully fabricated by this method. Here we reported that the In-doped ZnO nanorods successfully prepared by electrochemical deposition method. The influence of the preparation conditions on the morphology and optical properties was studied by changing the applied potential and adding different contents of indium into the ZnO.

2. Experimental

Electrochemical deposition process was carried out in aqueous electrolytes, which contained $Zn(NO_3)_2 \cdot 6H_2O$ (0.01 mol/L), $(CH_2)_6N_4$ (5 mmol/L) and KCl (0.1 mol/L). In order to incorporate the defined indium contents (In: Zn =0.5%, 1%, 1.5%, 3%) into ZnO lattice, calculated amount of $In(NO_3)_3$ was added to the deposition baths. In this experiment, the In-doped ZnO nanorods were prepared by a simple three-electrode cell. An ITO glass with 2.0 cm^2 as the substrate, was used as the working electrode in the three-electrode cell, while a Pt foil as the counter electrode, and a silver chloride electrode (Ag/AgCl) as the reference electrode. Before the start of the preparation, the ITO glass was cleaned in ethanol, acetone, deionized water by

ultrasound, respectively, then, immersed in HCl (0.1mol/L) for 30s before rinsing by deionized water again. The preparation of In-doped ZnO was carried out on the cleaned ITO glass under 80°C. Fig. 1 shows a scheme of the electrochemical reaction cell. In order to control shapes of In-doped ZnO nanorods, two applied potentials of -1.1V, -1.2V were applied for 40 min. The illustration of electrodeposition of In-doped ZnO nanorods on ITO glass is depicted in Fig. 2.

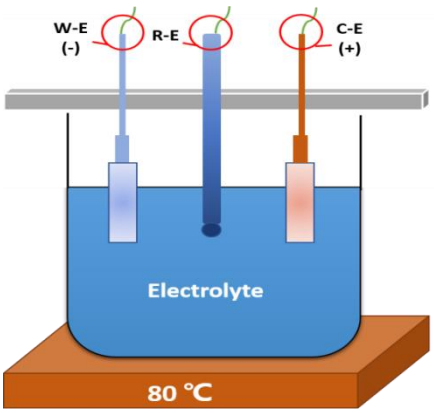

Fig. 1. Scheme of the electrochemical reaction cell

Field emission scanning electron microscopy (FESEM; UItra-55), X-ray diffraction (XRD; D/Max 1400), and high-resolution transmission electron microscopy (HRTEM; Libra200) with selected–area electron diffraction (SAED) analyses were used to study crystalline structures and morphologies of nanorods arrays. For HRTEM observations, the prepared In-doped ZnO were separated from the ITO glass substrate and suspended in ethanol solution, then ultrasound for 10 min. The chemical composition of the In-doped ZnO nanorods was determined by an energy dispersive spectrometer (EDS; Genesis-60s). Photoluminescence (PL; LS-55) spectra was used to measure the optical properties of the In-doped ZnO nanorods coated on ITO glass substrate by a He-Cd laser of 325 nm excitation wavelength at room temperature.

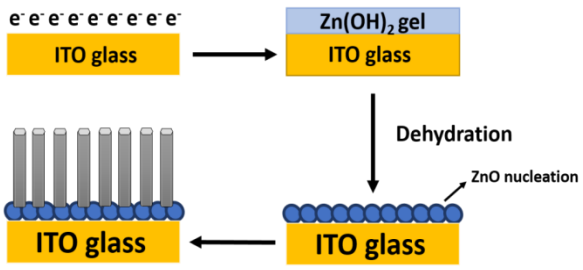

Fig. 2. Schematic illustration of In-doped ZnO nanorods grown on the ITO glass substrate by electrodeposition route

3. Result and discussion

In-doped ZnO nanorods were prepared in solution of 0.01 mol/L $Zn(NO_3)_2 \cdot 6H_2O$, 0.005 mol/L $(CH_2)_6N_4$, 0.1 mol/L KCl and different indium concentrations with two different applied potentials of -1.1V, -1.2V for 40 min. Fig. 3 shows the morphology of the In-doped ZnO nanorods. Fig. 3(f) shows profiles of those ZnO nanorods are all the hexagonal structure. The side length of the hexagon is in the order of 120 nm and the diameters of prepared nanorods are 180-250 nm as shown in Fig. 3(a). With the indium contents up to 1%, these nanorods didn't have remarkable changes in morphology and size, as shown in Fig. 3(b). After increasing the contents of indium to 1.5%, the dimension of nanorods didn't change significantly, but with slight agglomeration as shown in Fig. 3(c). When the content of the indium increased to 3%, an obvious change in size and morphology was observed in Fig. 3(e). The diameters of ZnO doped with 3% indium nanorods are about 150-200 nm with an obvious agglomeration. When the contents of indium increases, the In-doped ZnO nanorods have more obviously agglomerations and smaller size, which indicating the doping can promote grain refinement. Due to increasing concentration of indium, the relative concentration of grain surface is increased, diffusion barrier and diffusion activation energy of the crystal surface also increased, so that diffusion movement of the grain boundary is hindered and rate of crystal growth is slowed down as well. The main reason of hindered movement and slowed growth was due to the decreased size of In-doped ZnO nanorods and agglomerations of the nanorods. Fig. 3(d) shows the diameters of prepared nanorods are about 20-250 nm, the heterogeneity in size distribution is caused by the energy available for the In-doped ZnO growth is low under relatively low deposition potential, which resulted in a decreased nuclei per unit time and a more dispersed nanorods.

Fig. 4 shows EDS spectra results of the prepared In-doped ZnO nanorods. The peaks of Zn were observed at 1.0 and 8.7 keV while the indium signals at 0.5 and 3.4 keV. The silicon and gold signals in figure 4 were originated from silicon dioxide film on the surface of ITO glass substrate and sputter gold in the SEM measurement. The composition analysis revealed that the indium contents were about 0.55, 0.97, 1.58 and 2.92 at.% incorporated into the ZnO lattice as shown in Fig. 4(a)-(d).

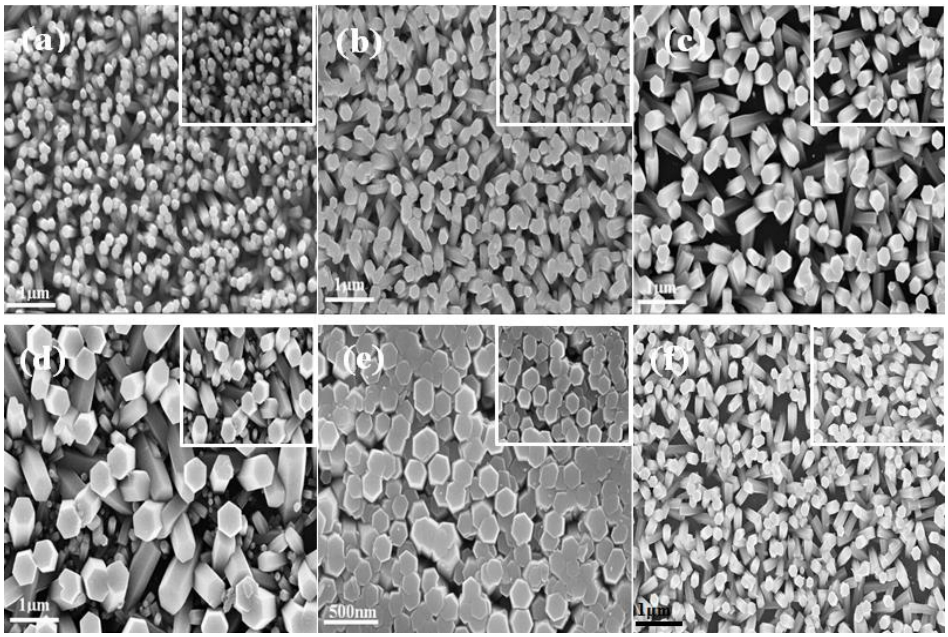

Fig. 3. SEM images of In-doped ZnO nanorods grown on the ITO glass substrate. The corresponding applied potentials and contents of indium: (a) -1.2 V, 0.5%, (b) -1.2 V, 1%, (c) -1.2 V, 1.5%, (d) -1.1 V, 1.5%, (e) -1.2 V, 3%, (e) -1.2 V, 0%. Preparing conditions: t = 40 min, T = 80 ℃

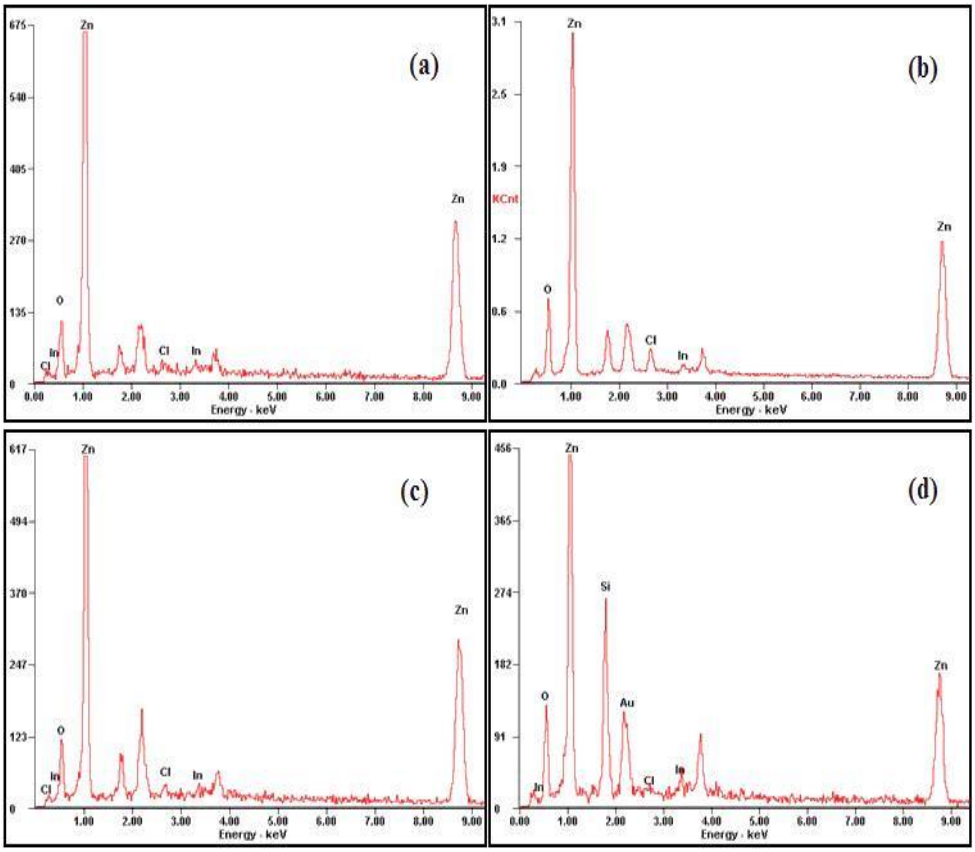

Fig. 4. EDS spectrum of the In-doped ZnO nanorods grown on ITO glass substrate. The corresponding contents of indium: (a) 0.5%, (b) 1%, (c) 1.5%, (d) 3%

XRD spectra of the In-doped ZnO with different contents of indium and deposition potentials were shown in Fig. 5. The major diffraction peaks are all of wurtzite-structured ZnO in agreement with JCPDS card (No. 36-1451). In the spectra we can observe the In-doped ZnO nanorods represent a relatively strong diffraction peak on the (002) plant, this means that In-doped ZnO nanorods along the [0001] direction have the advantage of growth orientation. By increasing the contents of indium, the intensity of (002) peak gradually decreased and the [0001] direction preferential growth reduced. Moreover, a lower angle shift appeared by increasing the contents of indium: the (002) peak shifted from 34.55° to 34.22° with increasing contents of indium from 0 to 3.0%. This might be due to the change of lattice constant of ZnO as the radius of In ions (0.081 nm) is greater than that of Zn ions (0.074 nm) [29]. From EDS and XRD results, we believe that different contents of indium had entered into the ZnO lattices. By decreasing the deposition potential, the intensity of (002) peak reduced obviously. Also, a relatively lower deposition potential might lead to a poorly crystallinity of ZnO nanorods.

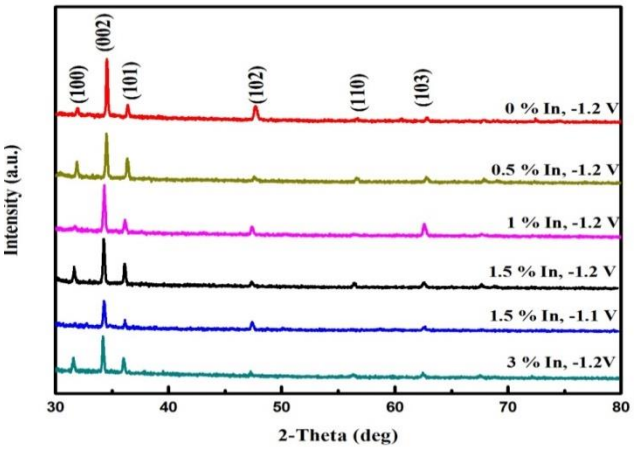

Fig. 5. XRD patterns for In-doped ZnO

The TEM and HRTEM images of the ZnO doped with 0.5% indium nanorods as shown in Fig. 6. In the Fig. 6(a) we can observe the diameters of prepared In-doped ZnO nanorod with the indium contents of 0.5% is about 180 nm. The HRTEM image shows that the lattice space 0.26 nm, matched the (0002) lattice spacing of ZnO. So the prepared nanorods obtained the preferential growth along [0001] direction. The selected-area electron diffraction (SAED) was used for further characterize of In-doped ZnO nanorods. The SAED image in the inserted Fig. 6(b) indicates that the In-doped ZnO nanorod prepared on the ITO glass substrate contains single crystals and along the [0001] direction has the advantage of growth orientation. The above results demonstrated that the indium ions have incorporated in the wurtzite nano-ZnO lattice successfully.

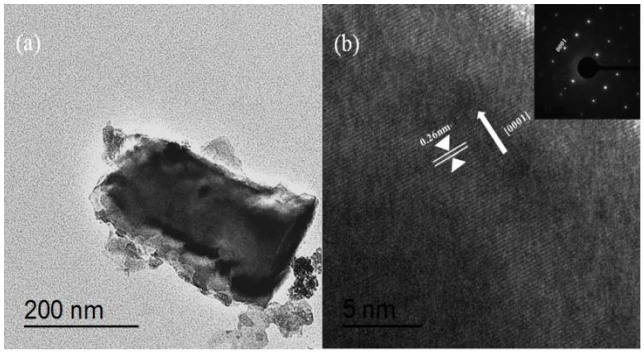

Fig. 6. (a) TEM (b) HRTEM image of In-doped ZnO nanorod with 0.5% contents of indium

In order to study the effect of doped indium contents, photoluminescence (PL) spectra was used to characterize optical properties of the In-doped ZnO nanorods coated on ITO glass substrate as shown in Fig. 7. The near band edge emission of the In-doped ZnO at about 372 nm was caused by the recombination of free excitons (band to band transition O 2p to Zn 3d) through an exciton-exciton collision process [30]. When increasing the contents of indium from 0% to 1.5%, the peak positions at about 371 nm red shift to 376 nm. However, it should be noted that an obvious red shift of increasing contents of indium from 1.5 to 3.0%, the peak positions at 376 nm shift to 390 nm, which may be synergies due to lattice defects and the nanorods agglomeration. Moreover, the intensities of the peak at about 371 nm are reduced and contents of indium, which may cause by the near band gap emission was suppressed by half-height width are broadened by increasing the increased contents of indium.

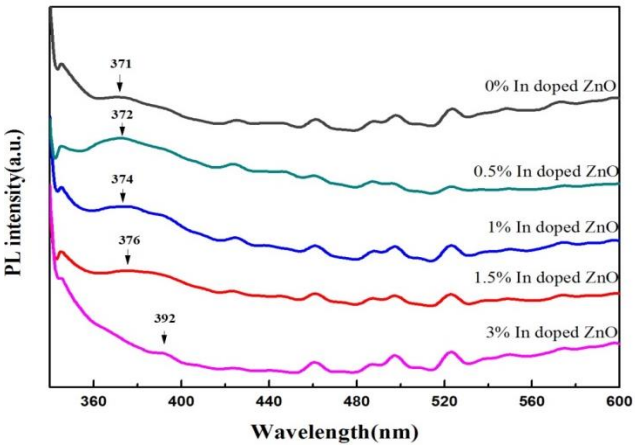

Fig. 7. Photoluminescence spectra of the In-doped ZnO nanorods coated on ITO glass substrate at different contents of indium

4. Conclusions

In summary, In-doped ZnO nanorods on the ITO glass substrate were successfully obtained by electrochemical

deposition route. The electrochemical deposition method represents high-efficiency, controllable, low energy -consumption and simplicity of operator for the preparation of In-doped ZnO. The morphology and size of the nanorods were studied by controlling contents of indium and the deposition potentials. The results of EDX and XRD both proved that these prepared nanorods on the ITO glass substrates are indeed composed of wurtzite structure In-doped ZnO crystals. The HRTEM and SAED revealed that the prepared In-doped ZnO nanorods obtained the preferential growth along [0001] direction and those nanorods consist of single crystals. The PL spectra of In-doped ZnO nanorods coated on ITO glass substrate appeared markedly red-shifted by increasing contents of indium at the peak about 371 nm. Because of the special optical properties, the prepared In-doped ZnO nanorods may be applied in the photocatalysis devices and optical protecting coatings. The mechanism of optical synergies of indium and ZnO needs further studies.

References

[1] D. Jassby, B. J. Farner, M. Wiesner, Environ. Sci. Techno. **46**, 6934 (2012).
[2] S. Xu, W. Guo, S. Du, M. M. Loy, N. Wang, Nano. Lett. **12**, 5802 (2012).
[3] T. Gruber, C. Kirchner, R. Kling, F. Reuss, A. Waag, Appl. Phys. Lett. **84**, 5359 (2004).
[4] S. A. Ansari, M. M. Khan, M. O. Ansari, J. Lee, M. H. Cho, J. Am. Chem. Soc. **117**, 27023 (2013).
[5] G. Tang, S. Tian, Z. Zhou, Y. Wen, A. Pang, Y. Zhang, D. Zeng, H. Li, B. Shan, C. Xie, J. Phys. Chem. C **118**, 11833 (2014).
[6] Y. Li, X. Zhao, W. Fan, J. Phys. Chem. C **115**, 3552 (2011).
[7] K. S. Jeong, S. K. Oh, H. S. Shin, H. J. Yun, S. H. Kim, H. R. Lee, K. M. Han, H. Y. Park, H. D. Lee, G. W. Lee, Jpn. J. Appl. Phys. **53**, 04 (2014).
[8] N. S. Karan, D. D. Sarma, R. M. Kadam, N. Pradhan, J. Phys. Chem. Lett. **1**, 2863 (2010).
[9] B. Chavillon, L. Cario, A. Renaud, F. Tessier, F. Cheviré, M. Boujtita, Y. Pellegrin, E. Blart, A. Smeigh, L. Hammarström, J. Am. Chem. Soc. **134**, 464 (2012).
[10] N. P. Herring, L. S. Panchakarla, M. S. El-Shall, Langmuir **30**, 2230 (2014).
[11] G. Kaur, A. Mitra, K. L. Yadav, Prog. Nat. Sci.-Mater. **25**, 12 (2015).
[12] Y. B. Lu, Y. Dai, M. Guo, L. Yu, B. Huang, Chem. Chem. Ph. **15**, 5208 (2013).
[13] C. Jang, Q. Jiang, J. Lu, Z. Ye, Structural, J. Mater. Sci. Techno. **31**, 1108 (2015).
[14] X. H. Lu, G. R. Li, W. X. Zhao, Y. X. Tong, Electrochimica Acta **53**, 5180 (2008).
[15] M. M. Ba-Abbad, A. A. H. Kadhum, A. B. Mohamad, M. S. Takriff, K. Sopian, Chemosphere **91**, 1604 (2013).
[16] R. Mohan, K. Krishnamoorthy, S. J. Kim, Solid State Commun. **152**, 375 (2012).
[17] X. Cai, Y. Cai, Y. Liu, H. Li, F. Zhang, Y. Wang, J. Chem. Phys. **74**, 1196 (2013).
[18] Y. Lu, Y. Lin, T. Xie, S. Shi, H. Fan, D. Wang, Nanoscale **4**, 6393 (2012).
[19] W. W. Li, Z. G. Hu, J. D. Wu, J. Sun, M. Zhu, Z. Q. Zhu, J. H. Chu, J. Phys. Chem. C **113**, 18347 (2009).
[20] S. J. Young, C. C. Yang, L. T. Lai, J. Electrochem. Soc. **164**, B3013 (2017).
[21] S. J. Young, Y. H. Liu, IEEE. T. Electron. Dev. **63**, 3160 (2016).
[22] Y. H. Liu, S. J. Chang, S. J. Young, ECS J. Solid. State. Sc. **5**, R203 (2016).
[23] O. Lupan, V. Cretu, V. Postica, M. Ahmadi, B. R. Cuenya, L. Chow, I. Tiginyanu, B. Viana, T. Pauporté, R. Adelung, Sensor. Actuat. B-Chem. **223**, 893 (2016).
[24] N. D. Dung, T. S. Cao, P. V. Loc, N. H. Cuong, P. T. Kien, P. T. Huy, N. N. Ha, J. Alloy. Compd. **668**, 87 (2016).
[25] J. W. Hoon, K. Y. Chan, J. Krishnasamy, T. Y. Tou, D. Knipp, Appl. Surf. Sci. **257**, 2508 (2011).
[26] C. Marin, V. Mihalache, S. E. Corina, R. Trusca, V. Bercu, L. Diamandescu, Superlattice. Microst. **104**, 2235 (2017).
[27] J. Sun, T. Zhao, Z. Ma, M. Li, C. Chang, H. Liang, J. Bian, C. Li, J. Phys. D. Appl. Phys. **48**, 456 (2015).
[28] J. Jie, G. Wang, X. Han, Q. Yu, Y. Liao, G. Li, J.G. Hou, Chem. Phys. Lett. **387**, 466 (2004).
[29] M. Suja, S. B. Bashar, M. M. Morshed, J. Liu, Acs. Appl. Mater. Inter. **7**, 8894 (2015).
[30] P. Soundarrajan, M. Sampath, T. Logu, K. Sethuraman, K. Ramamurthi, Mater. Lett. **162**, 191 (2016).

*Corresponding author: Daiyt2003@163.com